Int. J. Electrochem. Sci., 15 **(2020)** 7082 – 7092, doi: 10.20964/2020.03.96

International Journal of
ELECTROCHEMICAL
SCIENCE
www.electrochemsci.org

Effect of Graphene Addition on Anticorrosion Performance of Two Kinds of Epoxy Coatings

Shuai Wang[1], *Rui Ding*[1], *Xiaodong Zhao*[1,*], *Qiang Fu*[1], *Hao Sun*[1] , *Shuyue Chen*[1], *Zhongyi An*[1], *Yan Li*[2], *Xinlei Qu*[3]

[1] School of Ocean, Yantai University, Yantai 264005, China;
[2] Qingdao Branch of Naval Aeronautical Engineering Academy, Qingdao 266041, China;
[3] Shandong Nanshan Aluminum Co., Ltd., Yantai 265706, China
[*]E-mail: danielxdzhao@aliyun.com

Received: 22 October 2019 / *Accepted:* 9 January 2020 / *Published:* 10 June 2020

Graphene is a kind of two-dimensional lamellar nano-material with excellent barrier property, and it has important application in the field of anticorrosive coatings. The effect of graphene addition on the corrosion resistance of zinc-rich epoxy coating and glass flake epoxy coating was investigated by open-circuit potential(E_{ocp}), AC impedance and corrosion morphology. The results showed that the radius of arc resistance of epoxy zinc-rich coating with graphene was smaller than that of epoxy zincrich coating without graphene. The arc resistance with epoxy glass flake coating decreased gradually in 528h. It showed from the corrosion morphology observation that the addition of graphene improved the corrosion resistance of the zinc-rich coating, but reduced the corrosion resistance of the epoxy glass flake coating.

Keywords: Graphene; Epoxy zinc-rich coating; Epoxy glass flake coating; Electrochemical analysis

1. INTRODUCTION

The construction of engineering facilities in coastal areas will inevitably be involved with the corrosion due to the changeable coastal climate, high humidity and large amount of corrosive chloride ions and salts in the atmosphere. It not only causes significant economic losses, but also brings serious threat to personal safety and ecological environment. Especially some localized corrosion such as corrosion perforation or stress corrosion cracking occurs suddenly and causes safety accidents. Compared with other materials and construction technology, organic coating has become the most widely used anti-corrosion technology for its advantages of excellent performance, convenient construction and relatively low price[1]. At present, there are many problems needed to be solved urgently with epoxy zinc-rich and other heavy-duty anticorrosive coatings, such as serious pollution, low filler utilization rate and poor construction performance. As a functional filler with low

environmental risk, graphene is often added into anticorrosive coatings for the preparation of environment-friendly and excellent composite anticorrosive coatings[2-4].

Graphene is a kind of two-dimensional carbon nano-material with hexagonal honeycomb lattice composed of carbon atoms with sp^2 hybrid orbitals, and it has excellent electrical and optical properties. A great deal of research has been carried out on the effect of graphene on the corrosion resistance of metals and coatings, and graphene has been proposed and tested as a potential coating material to prevent corrosion[5-6]. Zhang[7] found that three layers of graphene effectively improved the oxidation resistance and electrochemical corrosion resistance of the material. Chen[8] studied the composite anticorrosive coating of graphene/organosiloxane modified resin and found that the addition of graphene significantly improved the anticorrosive performance of the composite coating. Liu[9] studied the effect of dispersed graphene on the corrosion resistance of epoxy coating. Compared with pure epoxy coating, graphene composite coating showed excellent barrier performance for H_2O molecules. Nurul[10] found that graphene protected metals from oxidative corrosion by creating highly zigzag pathways to prevent the diffusion of oxygen and water molecules to the surface of metal-based materials. Raghupathy[11] found that the improvement of corrosion resistance of copper could be attributed to the fact that graphene oxide prevented the diffusion of Cu^{2+} through the cross section of the coating to make the coating highly impermeable. Kumar[12] found that the combination of graphene and zinc-iron matrix improved the corrosion resistance of the coating, and graphene played a synergistic role. The degree of corrosion resistance of graphene films varied greatly. Schriver[13] found that although graphene provided an effective short-term oxidation protection, it promoted more extensive wet corrosion than the initially exposed unprotected copper surface over a longer time scale.

However, the influence of graphene addition on the corrosion performance of the coatings studied by many researchers was relatively single for most of them were focused on epoxy zinc-rich coatings. It was generally believed that the epoxy zinc-rich coating provided good sacrificial anode protection in the early stage, while in the later stage, the alkaline and low solubility of zinc corrosion products provided additional barrier protection[14]. However, the effect of graphene on the anticorrosive properties of different coatings was rarely studied. The interior of the glass scale coating is parallel and overlapped, which can prolong the time when the corrosion ions penetrating the coating, thus delaying the corrosion[15]. In this study, graphene as a dispersive slurry was added into two coating systems, epoxy zinc-rich coating and epoxy glass flake coating. The effects of graphene on the corrosion resistance of the two coating systems were investigated through the analysis of open circuit potential, AC impedance and corrosion morphology.

2. EXPERIMENTAL SECTION

2.1. Material

The chemical composition (wt.%) of the Q235 steel used in the experiment is as follows: C 0.18, Si 0.18, Mn 0.36, P 0.016, S 0.008, Al 0.011, Fe margin.

The working face of the sample was cut with a square working area of 1 cm^2, and the nonworking surface was welded with a copper wire, and then sealed with an epoxy resin and polytriethylene tetramine. Before the experiment, the working surface of each sample was polished with 200 to 1000# sandpaper, washed with distilled water and ethanol, and dried for use.

Epoxy zinc-rich paint and epoxy glass flake paint were provided by Zhejiang Feijing New Material Co., Ltd. The graphene and dispersant slurry were provided by Sinopec Research Institute of Safety Engineering.

2.2. Coating Preparation

Every 99.5g original anticorrosive coating system together with 0.5g graphene and dispersant slurry were mixed respectively and stirred until well mixed, used as graphene composite coating system. Four groups of Q235 steel electrodes were covered by epoxy zinc-rich paint, graphene/epoxy zinc-rich paint, epoxy glass flake paint, graphene/epoxy glass flake paint on the working surface, respectively, and marked as sample A, A_G, B, B_G. After the dry film of the coatings were completely formed, a hole was made artificially on the coating surface in order to accelerate the corrosion process.

2.3. Electrochemical measurement and corrosion morphology analysis

All electrochemical tests were carried out on the electrochemical workstation (PARSTAT2273, USA). The classic three electrode system was adopted, the Q235 steel electrode with coating was used as working electrode, a platinum-niobium wire with a diameter of 4 mm used as the counter electrode, and a saturated calomel electrode (SCE) as the reference electrode. After stabilization of the system, the open circuit potential was measured at each interval. Electrochemical impedance spectroscopy (EIS) was carried out in the frequency range of 10^{-2}-10^5 Hz and the amplitude of the sinusoidal voltage signal was 10 mV. The data were analyzed and processed by ZSimpWin, C-View and Origin software.

During the experiment, all samples were immersed in 3.5% NaCl solution. After the end of the experiment, the surface morphology of the samples were observed under the stereomicroscope.

3. RESULTS AND DISCUSSION

3.1. OCP measurement

Fig.1 and 2 show E_{ocp} of the samples A, A_G, B and B_G immersed in 3.5% NaCl solution over time.

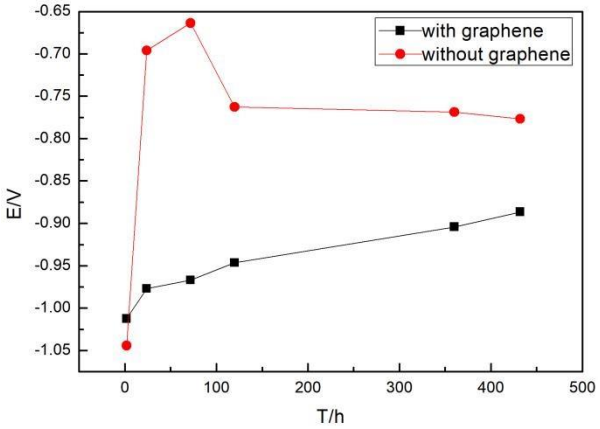

Figure 1. E_{ocp} of Q235 steel with epoxy zinc-rich coating and graphene/epoxy zinc-rich coating during immersion in a 3.5% NaCl solution

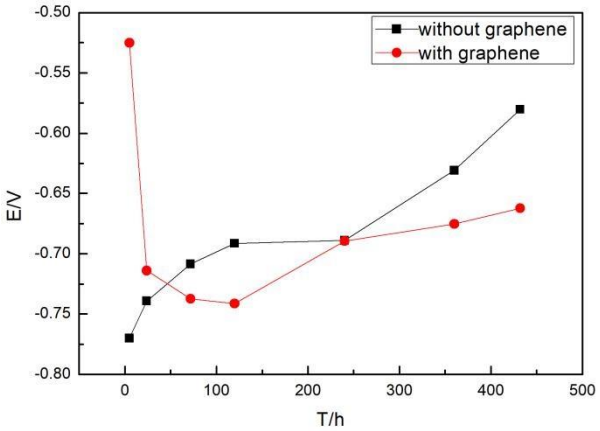

Figure 2. E_{ocp} of Q235 steel with epoxy glass flake coating and graphene/epoxy glass flake coating during immersion in a 3.5% NaCl solution

3.2. EIS measurement

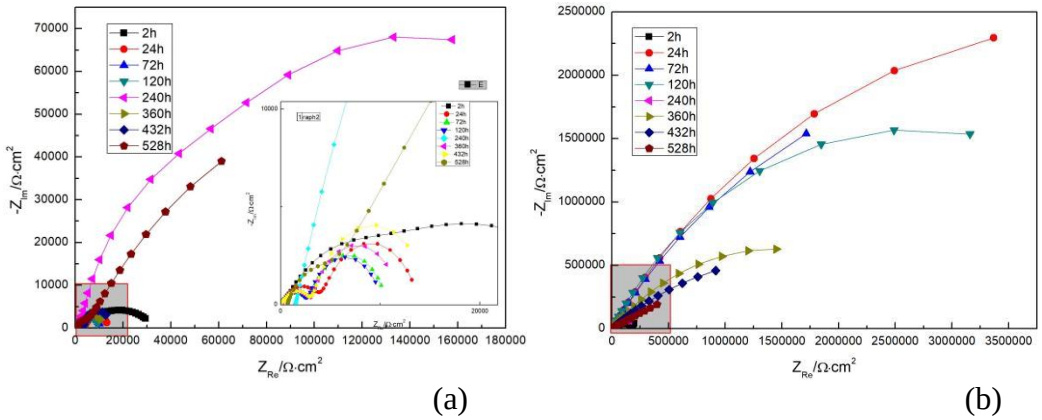

Figure 3. Nyquist diagrams of Q235 steel covered with epoxy zinc-rich coating (a)with or (b)without graphene addition immersed in 3.5% NaCl solution for 528h

As shown in Fig.1 and Fig.2, the potential of Q235 steel covered with epoxy zinc-rich coating shifted positively as a whole, and the potential of steel covered with graphene/epoxy zinc-rich coating was far lower than that of the coating without graphene. The steel potential of the epoxy glass coating without graphene shifted positively, while that of the graphene/epoxy glass coating showed a negative shift.

As shown in Fig.3, the Nyquist diagrams of both coatings showed a characteristic impedance semicircle controlled by charge transfer during the experimental period. During the period of 24-528h, the capacitive arc of the coating without graphene decreased, indicating that the corrosion tendency increased with time. The arc-resistance radius of Q235 steel with epoxy zinc-rich coating with graphene decreased at first and then increased later. It revealed that at the beginning of the experiment, artificial damage and good conductivity of graphene promoted the occurrence of corrosion. In the later stage, the increase of capacitive arc radius might be due to the formation of a product film on the surface of Q235 steel[16], which changed the state of the electrode surface and temporarily acted as a barrier. In contrast, the capacitive arc radius of the zinc-rich epoxy coating without graphene was much larger than that with graphene.

In order to show its impedance characteristics further, Zsimpwin software was used to fit the electrochemical impedance spectrum, and the equivalent circuit was shown in Fig.4. Where R_s represents the solution resistance, R_c represents the coating resistance, R_{ct} represents the charge transfer resistance, Q_c represents the capacitance of the organic layer in the coating, Q_{dl} represents the electric double layer capacitance, and Q is the constant phase element CPE. When n = 1, CPE = C, that is, the capacitance at this time is the ideal capacitance. The results of fitting parameters are shown in Table 1.

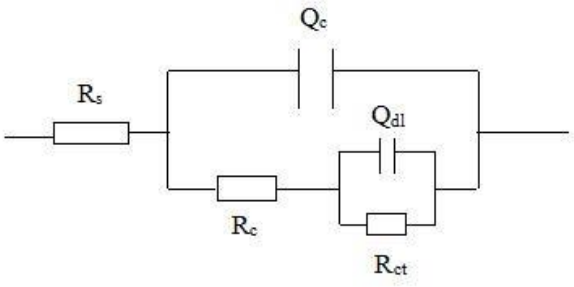

Figure 4. Equivalent circuit model used to fit the EIS experimental data for Q235 steel covered with epoxy zinc-rich coating with or without graphene immersed in 3.5% NaCl solution

Table 1. Fitting parameters derived from equivalent circuit model in Fig. 4

Sample No.	T (h)	R_s (Ω/cm^2)	$Q_c \times 10^{-7}$ (F/cm^2)	n_1	$R_c \times 10^3$ (Ω/cm^2)	$Q_{dl} \times 10^{-6}$ (F/cm^2)	n_2	$R_{ct} \times 10^4$ (Ω/cm^2)
A	2	100	5.62	0.33	239.1	7.93	0.73	4.76
	24	100.9	0.85	0.52	5.04	9.56	0.64	881.4
	72	1690	2.14	0.57	3.28	19.66	0.95	781.2
	120	151.6	0.04	0.73	4.06	8.82	0.67	536.3

	240	1460	2.05	0.75	124.3	97.11	0.74	12.79
	360	26.36	1.49	0.53	2844	0.49	0.76	0.76
	432	1.178E-2	2.28	0.42	3217	2.567E-7	0.8	1308
	528	5.319E-3	4.92	0.30	8.082E-4	0.32	0.75	827.8
A_G	2	1000	1.97	0.61	5.42	192.7	0.35	2.85
	24	25.53	124.5	0.72	9.82	31.49	0.53	0.42
	72	30.81	3.21	0.57	2.86	1539	0.73	0.78
	120	31.64	196.9	0.72	7.63	33.43	0.57	0.27
	240	1447	5.25	0.67	227.2	26.87	0.88	0.33
	360	44	4.65	0.53	3.05	2931	0.75	0.91
	432	48.86	267.9	0.76	12.01	52.72	0.52	0.32
	528	649.3	48	0.52	230.8	41.42	0.69	0.39

Tab.1 showed that the R_{ct} of epoxy zinc-rich coating with graphene decreased rapidly from 28450 $\Omega \cdot cm^{-2}$ to 4162 $\Omega \cdot cm^{-2}$ in 2-24 hours, indicating that the conductivity of graphene promoted the corrosion of zinc at the early stage of coating damage. In the experimental period, the R_{ct} of Q235 steel without graphene epoxy zinc-rich coating increased first, then decreased and increased at last, while that of Q235 steel with graphene epoxy zinc-rich coating increased first and then decreased, and the change range was smaller than that of epoxy zinc-rich coating. In general, the R_{ct} of zinc-rich epoxy coating without graphene was much larger than that of graphene coating, indicating that the addition of graphene accelerated the corrosion of zinc and slowed down the corrosion of Q235 steel substrate from a certain point of view.

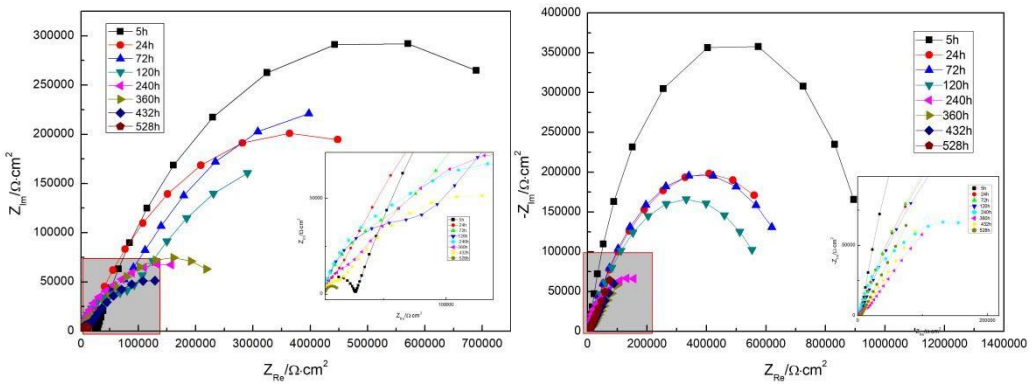

Figure 5. Nyquist diagram of Q235 steel covered with epoxy glass flake coating (a)with or (b)without graphene immersed in 3.5% NaCl solution for 528h

As shown in Fig.5, the Nyquist diagrams of both coatings showed a characteristic impedance semicircle controlled by charge transfer. In general, the R_{ct} of glass flake coating without graphene was larger than that of glass flake coating with graphene.

The electrochemical impedance spectrum was fitted with the equivalent circuit diagram shown in Fig. 6. The obtained fitting parameter values were listed in Table 2.

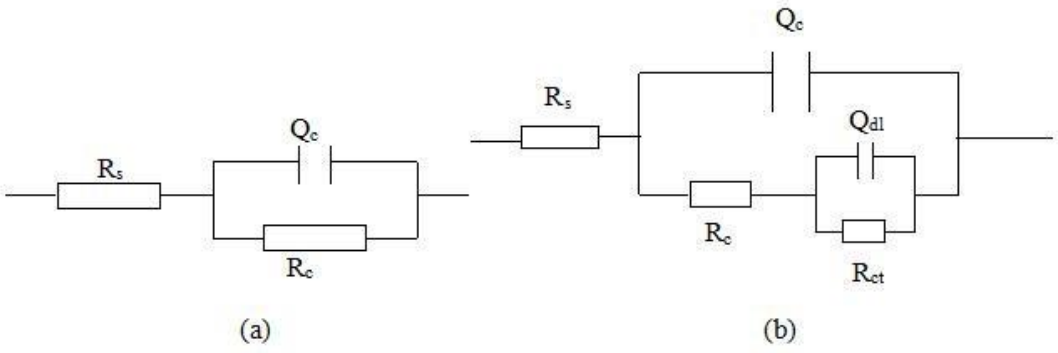

Figure 6. Equivalent circuit model used to fit the EIS experimental data for Q235 steel covered with epoxy glass flake coating immersed in 3.5% NaCl solution (The equivalent circuit a was used for 3h, 24h, 120h and 240h of Q235 steel covered with epoxy glass flake coating without graphene, and the equivalent circuit b was used for the rest.)

Table 2. Fitting parameters derived from equivalent circuit model in Fig. 6

Sample No.	t(h)	R_s (Ω/cm^2)	$Q_c \times 10^{-6}$ (F/cm^2)	n_1	R_c (Ω/cm^2)	$Q_{dl} \times 10^{-6}$ (F/cm^2)	n_2	R_{ct} (Ω/cm^2)
B	5	541.0	4.95	0.55	6637	2.04	0.82	971700
	24	1020	3.20	0.59	794000	--	--	--
	72	3057	2.18	0.61	756100	--	--	--
	120	3474	2.11	0.59	660100	--	--	--
	240	1420	2.65	0.71	194900	--	--	--
	360	2146	1.03	0.82	7972	26.56	0.41	973200
	432	4360	29.00	0.40	2.636E13	--	--	--
	528	0.01	6.28	0.22	5616	39.67	0.48	1.205E19
B_G	5	0.01	0.002	0.74	27410	4.05	0.70	96550
	24	484.8	5.89	0.64	729500	2.12	0.79	8164
	72	577.1	10.32	0.68	754200	2.58	0.72	65400
	120	815.2	15.50	0.64	623700	1.78	0.77	74140
	240	1447	5.25	0.67	227200	2.69	0.88	32830
	360	815.7	2.32	0.74	19830	9.95	0.63	276100
	432	792.1	19.45	0.56	217500	1.59	0.78	11580
	528	39.79	6.16	0.50	2275	246.2	0.74	13090

The fitting parameters showed that the R_{ct} of glass flake coating with graphene decreased rapidly from 96550 $\Omega \cdot cm^{-2}$ to 8164 $\Omega \cdot cm^{-2}$ in 5-24 hours. In general, the R_{ct} of glass flake coating without graphene was much larger than that without graphene.

3.3. Surface morphology

Fig.7 shows the surface morphology characteristics of the artificially damaged coating under the stereomicroscope after immersion in 3.5% NaCl solution for 528h.

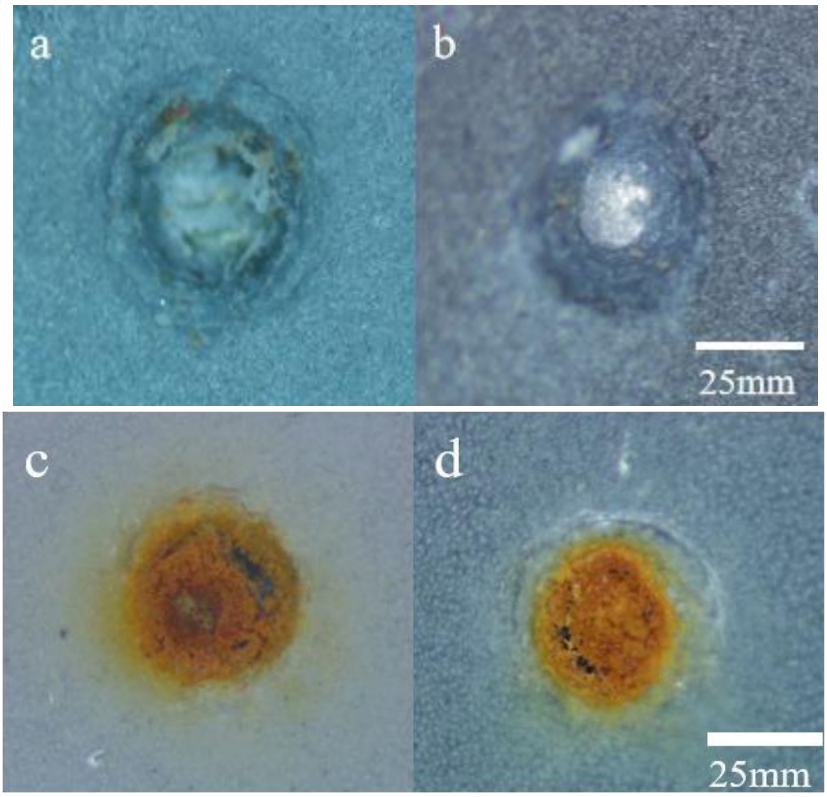

Figure 7. Corrosion morphology of Q235 steel covered with artificially damaged coatings after immersion in 3.5% NaCl solution for 528h (a) epoxy zinc-rich coating; (b) graphene/epoxy zinc-rich coating; (c) glass flake coating; (d) graphene/glass flake coating

As shown in the Fig.7, Q235 steel with different coating had different corrosion morphology after immersion for the same time. Compared with Fig.7(a) and (b), it showed that the epoxy zinc-rich coating without graphene developed yellow-brown corrosion product around the hole, which was significantly more than that with graphene, indicating that the corrosion was more severe. The addition of graphene improved the corrosion resistance of the epoxy zinc-rich coating, and it was consistent with the analysis of impedance results.

3.4. Discussion

For the epoxy zinc-rich coating, as shown in Fig.8, graphene sheet had a strong conductive effect, and the electrons lost in the anode reaction on the metal surface could be quickly transferred to the coating surface through the graphene sheet layer, so that the cathode electrons reacted directly within the coating surface[17-18]. The generated OH^- stayed on the surface of the epoxy zinc-rich coating and reacted with the zinc ion to generate zinc hydroxide precipitation from reacting with iron ions. The strong conductivity of graphene promoted the cathodic protection of zinc-rich epoxy coating, thus slowing down the corrosion of metal substrate.

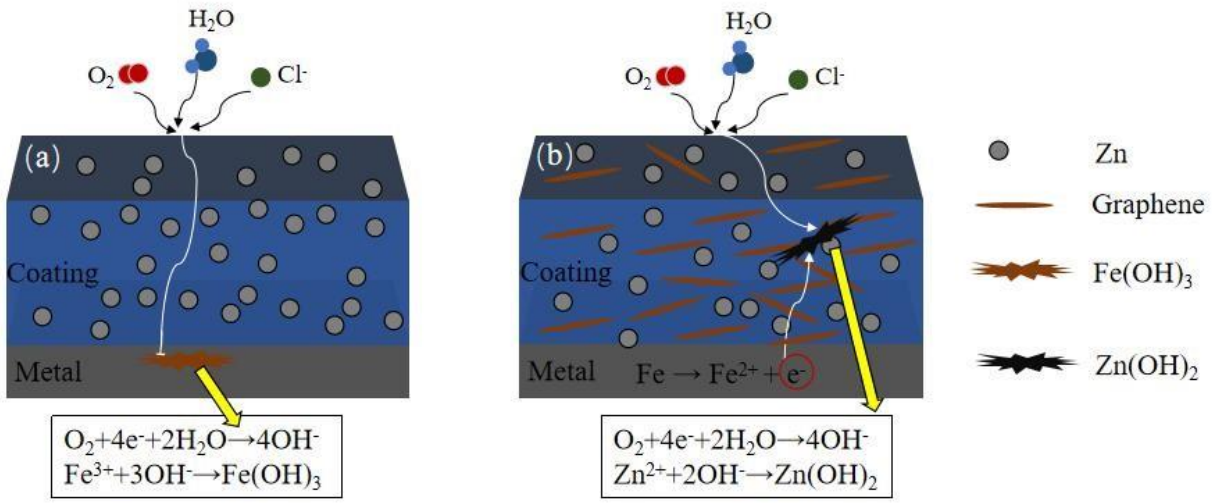

Figure 8. Schematic diagram of effect of graphene addition on epoxy zinc-rich coating (a) Epoxy zinc-rich coating; (b) Graphene/epoxy zinc-rich coating

For the epoxy glass flake coating, as shown in Fig.9, the excellent anti-corrosion function of the epoxy glass flake coating was mainly due to labyrinth effect, the unique shielding structure formed by the scale in the coating. That is, the shielding effect, which refers to the phenomenon that a fluid or gas has resistance through a scaly layered structure and reduces its flow rate[19]. However, graphene had a large specific surface area, and the strong interaction between π-π bond together with van der Waals force[20] enabled graphene in the substrate to aggregate easily[21]. The aggregation of graphene destroyed the "labyrinth effect" of the coating, providing channels for the corrosion factors such as water molecules, oxygen, and chloride ions to enter the coating and reach the metal substrate, which accelerated the corrosion of the metal.

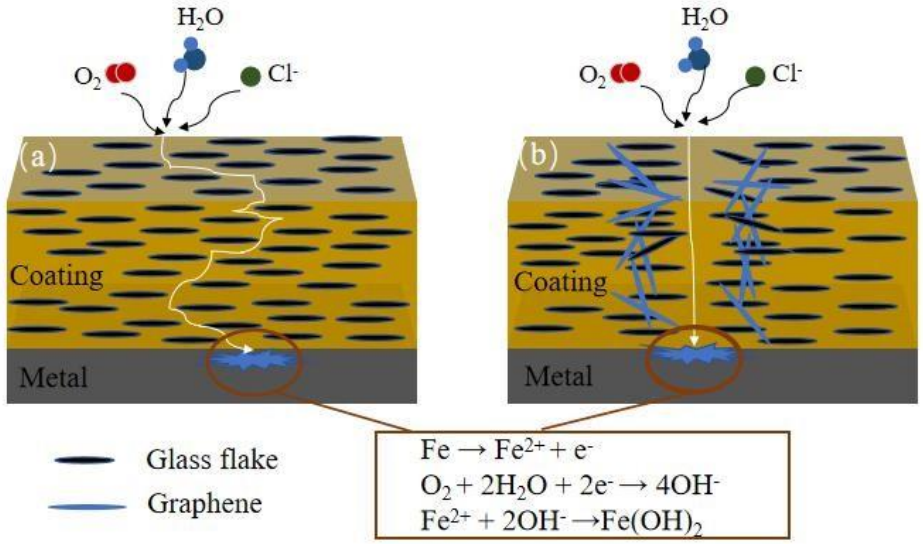

Figure 9. Schematic diagram of graphene effect of graphene addition on epoxy glass flake coating (a) Glass scale layer; (b) Graphene/Glass scale layer

4. CONCLUSION

The effects of graphene on the corrosion resistance of zinc-rich epoxy coating, conductive epoxy coating and glass flake coating were investigated by open circuit potential, AC impedance and corrosion morphology analysis. The main conclusions were as follows:

Although the radius of the capacitive reactance of Q235 steel with graphene/epoxy zinc-rich coating was significantly smaller than that of Q235 steel with epoxy zinc-rich coating, in view of the corrosion morphology, the corrosion was more severe for the coating with graphene addition. The conductivity of graphene promoted the cathodic protection of zinc-rich epoxy coating, thus protecting the metal substrate. However, when graphene was added to the glass flake coating, the strong interaction between π-π bond together with van der Waals force enabled graphene in the substrate to aggregate easily, which destroyed the "labyrinth effect" of the coating, provided channels for the corrosion factors and accelerated the corrosion of the metal.

ACKNOWLEDGMENTS
The work is supported by State Key Laboratory of Ocean Engineering(Shanghai Jiao Tong University)(Grant No.1912).

References

1. R. Ding, S. Chen and J. Lv., *Acta. Chim. Sinica.*, 806 (2019) 611.
2. J. H. Chi, S. Chen and X. F. Chen, *Equipm. Envir. Eng.*, 15 (2018) 62.
3. Y. Tong, S. Bohm and M. Song, *Appl. Surf. Sci.*, 424 (2017) 72.
4. R. Ding, Y. Zheng and H. Yu, *J. Alloy. Comd.*, 748 (2018) 481.

5. N. T. Kirkland, T. Schiller and N. Medhekar, *Corros. Sci.*, 56 (2012) 1.
6. D. Prasai, J. C. Tuberquia and R. R. Harl, *Acs. Nano.*, 6 (2012) 1102.
7. H. X. Zhang, Q. Ma and Y. Z. Wang, *New. Carbon. Mater.*, 34 (2019) 153.
8. Y. Chen, *Preparation and properties of graphene composite anticorrosive coating on carbon steel*, Anhui University of Technology, 2017.
9. S. Liu, L. Gu, H. C. Zhao and J. M. Chen, *J. Mater. Sci. Technol.*, 32 (2016) 425.
10. H. O. Nurul and M. Mazli, *Prog. Org. Coat.*, 135 (2019) 82.
11. Y. Raghupathy, A. Kamboj and M. Y. Rekha, *Thin. Solid. Films.*, 636 (2017) 107.
12. M. K. Punith Kumar and M. Y. Rekha, *J. Alloy. Comd.*, 783 (2019) 820.
13. M. Schriver, W. Regan and W. J. Gannett, *Acs. Nano.*, 7 (2013) 5763.
14. S. Shreepathi, P. Bajaj and B. P. Mallik, *Electrochim. Acta*, 55 (2010) 5129.
15. S. Ackermann, M. Steimecke and C. Morig, *J. Electroanal. Chem.*, 795 (2017) 68.
16. T. Li, S. Qiu and Y. X. Bao, *Shanghai Coat.*, 57 (2019) 32.
17. A. A. Oskuie, T. Shahrabi and A. Shahriari, *Corros. Sci.*, 61 (2012) 111.
18. J. Luo, J. H. Wang and S. G. Wen, *Coat. Indus.*, 47 (2017) 69.
19. B. Jin, D. B. Xiong and Z. Tan, *Carbon*, 142 (2019) 482.
20. H. Alhumade, R. P. Nogueira and A. Yu, *Prog. Org. Coat.*, 122 (2018) 180.
21. H. X. Zhang, Q. Ma, Y. Z. Wang and B. S. Xu, *New. Carbon. Mater.*, 34 (2019) 153.

© 2020 The Authors. Published by ESG (www.electrochemsci.org). This article is an open access article distributed under the terms and conditions of the Creative Commons Attribution license (http://creativecommons.org/licenses/by/4.0/).